Hydrol. Earth Syst. Sci., 18, 3763–3775, 2014
www.hydrol-earth-syst-sci.net/18/3763/2014/
doi:10.5194/hess-18-3763-2014

Hydrology and Earth System Sciences
Open Access

Soil erosion by snow gliding – a first quantification attempt in a subalpine area in Switzerland

K. Meusburger[1], G. Leitinger[2], L. Mabit[3], M. H. Mueller[1], A. Walter[1], and C. Alewell[1]

[1]Environmental Geosciences, University of Basel, Basel, Switzerland
[2]Institute of Ecology, University of Innsbruck, Innsbruck, Austria
[3]Soil and Water Management & Crop Nutrition Laboratory, Joint FAO/IAEA Division of Nuclear Techniques in Food and Agriculture, International Atomic Energy Agency, Vienna, Austria

Correspondence to: K. Meusburger (katrin.meusburger@unibas.ch)

Received: 26 February 2014 – Published in Hydrol. Earth Syst. Sci. Discuss.: 28 March 2014
Revised: 28 July 2014 – Accepted: 7 August 2014 – Published: 26 September 2014

Abstract. Snow processes might be one important driver of soil erosion in Alpine grasslands and thus the unknown variable when erosion modelling is attempted. The aim of this study is to assess the importance of snow gliding as a soil erosion agent for four different land use/land cover types in a subalpine area in Switzerland. We used three different approaches to estimate soil erosion rates: sediment yield measurements in snow glide depositions, the fallout radionuclide ^{137}Cs and modelling with the Revised Universal Soil Loss Equation (RUSLE). RUSLE permits the evaluation of soil loss by water erosion, the ^{137}Cs method integrates soil loss due to all erosion agents involved, and the measurement of snow glide deposition sediment yield can be directly related to snow-glide-induced erosion. Further, cumulative snow glide distance was measured for the sites in the winter of 2009/2010 and modelled for the surrounding area and long-term average winter precipitation (1959–2010) with the spatial snow glide model (SSGM). Measured snow glide distance confirmed the presence of snow gliding and ranged from 2 to 189 cm, with lower values on the north-facing slopes. We observed a reduction of snow glide distance with increasing surface roughness of the vegetation, which is an important information with respect to conservation planning and expected and ongoing land use changes in the Alps. Snow glide erosion estimated from the snow glide depositions was highly variable with values ranging from 0.03 to 22.9 $\mathrm{t\,ha^{-1}\,yr^{-1}}$ in the winter of 2012/2013. For sites affected by snow glide deposition, a mean erosion rate of 8.4 $\mathrm{t\,ha^{-1}\,yr^{-1}}$ was found. The difference in long-term erosion rates determined with RUSLE and ^{137}Cs confirms the constant influence of snow-glide-induced erosion, since a large difference (lower proportion of water erosion compared to total net erosion) was observed for sites with high snow glide rates and vice versa. Moreover, the difference between RUSLE and ^{137}Cs erosion rates was related to the measured snow glide distance ($R^2 = 0.64$; $p < 0.005$) and to the snow deposition sediment yields ($R^2 = 0.39$; $p = 0.13$). The SSGM reproduced the relative difference of the measured snow glide values under different land uses and land cover types. The resulting map highlighted the relevance of snow gliding for large parts of the investigated area. Based on these results, we conclude that snow gliding appears to be a crucial and non-negligible process impacting soil erosion patterns and magnitude in subalpine areas with similar topographic and climatic conditions.

1 Introduction

While rainfall is a well-known agent of soil erosion, the erosive forces of snow movements are qualitatively recognised but quantification has not been achieved yet (Leitinger et al., 2008; Konz et al., 2012). Wet avalanches, in particular, can yield enormous erosive forces that are responsible for major soil loss (Gardner, 1983; Ackroyd, 1987; Bell et al., 1990; Jomelli and Bertran, 2001; Heckmann et al., 2005; Fuchs and Keiler, 2008; Freppaz et al., 2010) in the avalanche release area (Ceaglio et al., 2012), too.

Besides avalanches, another important process of snow movement affecting the soil surface is snow gliding (In der Gand and Zupancic, 1966). Snow gliding is the slow (millimetres to centimetres per day) downhill motion of a snowpack over the ground surface caused by the stress of its own weight (Parker, 2002). Snow gliding predominantly occurs on south-east to south-west-facing slopes with slope angles between 30 and 40° (In der Gand and Zupancic, 1966; Leitinger et al., 2008). Two main factors that control snow glide rates are (i) the wetness of the boundary layer between the snow and soil cover and (ii) the ground surface roughness determined by the vegetation cover and rocks (McClung and Clarke, 1987; Newesely et al., 2000). So far, only few studies have investigated the effect of snow gliding on soil erosion (Newesely et al., 2000; Leitinger et al., 2008). A major reason for this shortcoming is the difficulty in obtaining soil erosion rates caused by snow processes. In steep subalpine areas, soil erosion records (e.g. with sediment traps) are restricted to the vegetation period because avalanches and snow gliding can irreversibly damage the experimental design (Konz et al., 2012).

Recently, first physically based attempts to model the erosive force of wet avalanches were made (Confortola et al., 2012). No similar model exists for snow gliding. However, the potential maximum snow glide distance during a targeted period can be modelled with the empirical spatial snow glide model (SSGM) (Leitinger et al., 2008). The modelling of this process is crucial in evaluating the impact of the snow glide process on soil erosion on a larger scale.

Soil erosion rates can be obtained by direct quantification of sediment transport in the field, by fallout-radionuclide (FRN)-based methods (e.g. Mabit et al., 1999; Benmansour et al., 2013; Meusburger et al., 2013) and by soil erosion models (Nearing et al., 1989; Merritt et al., 2003). Since the end of the 1970s empirical soil erosion models such as the Universal Soil Loss Equation (USLE; Wischmeier and Smith, 1965, 1978) and its refined versions, the Revised USLE (RUSLE; Renard et al., 1997) and the Modified USLE (MUSLE; Smith et al., 1984), have been used worldwide to evaluate soil erosion magnitude under various conditions (Kinnell, 2010). These well-known models allow the assessment of sheet erosion and rill/inter-rill erosion under moderate topography. However, they do not integrate erosion processes associated with wind, mass movement, tillage, channel or gully erosion (Risse et al., 1993; Mabit et al., 2002; Kinnell, 2005), and snow impact due to movement is not considered either (Konz et al., 2009). Several models have been tested for steep alpine sites with the result that RUSLE reproduced the magnitude of soil erosion, the relative pattern and the effect of the vegetation cover most plausibly (Konz et al., 2010; Meusburger et al., 2010b; Panagos et al., 2014). The erosion rate derived from RUSLE corresponds to water erosion induced by rainfall and surface runoff and, hence, in our site, to the soil erosion processes during the summer season without significant influence of snow processes.

In contrast, the translocation of FRN reflects all erosion processes by water, wind and snow during summer and winter season and, thus, is an integrated estimate of the total net soil redistribution rate since the time of the fallout in the 1950s (the start of the global fallout deposit) and, in the case of predominant Chernobyl ^{137}Cs input, since 1986. Anthropogenic fallout radionuclides have been used worldwide for decades to assess the magnitude of soil erosion and sedimentation processes (Mabit and Bernard, 2007; Mabit et al., 2008; Matisoff and Whiting, 2011). The most well-known conservative and validated anthropogenic radioisotope used to investigate soil redistribution and degradation is ^{137}Cs (Mabit et al., 2013).

For (sub-) alpine areas the different soil erosion processes captured by RUSLE and the ^{137}Cs method result in different erosion rates (Konz et al., 2009; Juretzko, 2010; Alewell et al., 2014; Stanchi et al., 2014). However, this difference might also be due to several other reasons, such as the error of both approaches, the non-suitability of the RUSLE model for this specific environment and/or the erroneous estimation of the initial fallout of ^{137}Cs.

In this study, we aim to quantify snow-glide-induced erosion and investigate whether the observed discrepancy between erosion rates estimated with RUSLE and the ones provided by the ^{137}Cs method can be at least partly attributed to snow gliding processes. Since vegetation cover affects snow gliding, four different subalpine land use/land cover types were investigated. A further objective of our research is to assess the relevance of snow gliding processes on a catchment scale using the spatial snow glide model (SSGM).

2 Materials and methods

2.1 Site description

The study site is located in central Switzerland (Canton Uri) in the Ursern Valley (Fig. 1). The elevation of the W–E extended alpine valley ranges from 1400 up to 2500 m a.s.l. At the valley bottom (1442 m a.s.l.), average annual air temperature for the years 1980–2012 is around 4.1 ± 0.7 °C and the mean annual precipitation is 1457 ± 290 mm, with 30 % falling as snow (data from MeteoSwiss). The valley is snow-covered from November to April with a mean annual snow height of 67 cm in the period 1980 to 2012. Drainage of the basin is usually controlled by snowmelt from May to June. An important contribution to the flow regime takes place during early autumn floods. Land use is characterised by hayfields near the valley bottom (from 1450 to approximately 1650 m a.s.l.) and pasturing further upslope. Siliceous slope debris and moraine material is dominant at our sites, and forms Cambisols (Anthric) and Podzols (Anthric) classified according to IUSS Working Group (2006).

Of the 14 experimental sites, 9 are located on the south-facing slope and 5 on the north-facing slope at altitudes

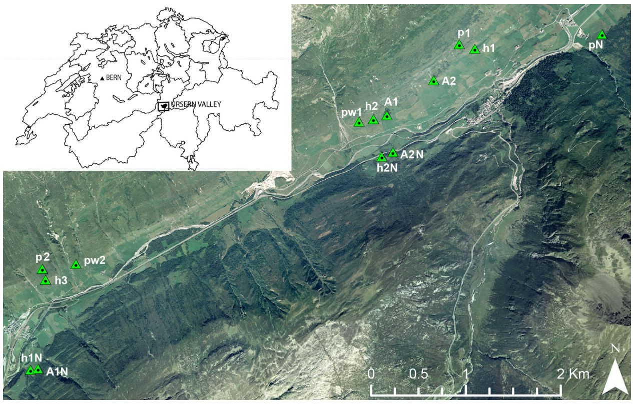

Figure 1. The Ursern Valley in the central Swiss Alps and the location of the 14 investigated sites (hayfields – h; pastures – p; pastures with dwarf shrubs – pw; and abandoned grassland covered with *Alnus viridis* – A; north-facing slope – N).

between 1476 and 1670 m a.s.l. Four different land use/land cover types with three to five replicates each were investigated: hayfields (h), pastures (p), pastures with dwarf shrubs (pw) and abandoned grassland covered with *Alnus viridis* (A). The vegetation of hayfields is dominated by *Trifolium pratense*, *Festuca* sp., *Thymus serpyllum* and *Agrostis capillaris*. For the pastured grassland, *Globularia cordifolia*, *Festuca* sp. and *Thymus serpyllum* dominate. Pastures with dwarf shrubs are dominated by *Calluna vulgaris*, *Vaccinium myrtillus*, *Festuca violacea*, *Agrostis capillaris* and *Thymus serpyllum*. At the pasture sites of the south-facing slope, which are stocked from June to September, cattle trails transverse to the main slope direction.

2.2 Snow glide measurement

We measured cumulative snow glide distances with snow glide shoes for the winter of 2009/2010. The snow glide shoe equipment was similar to the set-up used by In der Gand and Zupancic (1966), Newesely et al. (2000) and Leitinger et al. (2008). The set-up consisted of a glide shoe and a buried weather-proof box with a wire drum. Displacement of the glide shoe causes the drum to unroll the wire. The total unrolled distance was measured in spring after snowmelt. To prevent entanglement with the vegetation, the steel wire was protected by a flexible plastic tube. For each site, three to five snow glide shoes were installed to obtain representative values. A total of 60 devices were used.

2.3 Assessment of soil redistribution

Snow glide distance was measured with snow glide shoes for 14 sites. For 12 of the 14 sites (exclusive of the two *Alnus viridis* sites on the north-facing slopes (AN)), RUSLE- and ^{137}Cs-based erosion rates were assessed. Seven of these sites were measured in 2007 (Konz et al., 2009). During a second field campaign performed in 2010, five additional sites were investigated using the same methods for soil erosion assessment with ^{137}Cs and RUSLE as in 2007 (Konz et al., 2009). The ^{137}Cs measurements were decay-corrected to 2007 for comparison purposes.

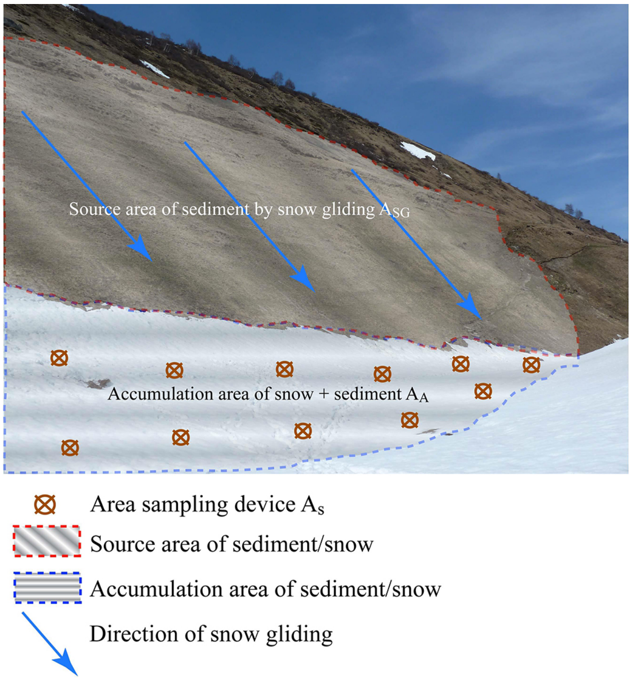

Figure 2. Illustration of the procedure for snow-glide-related erosion rate assessment.

2.3.1 Snow and sediment sampling in the snow glide deposition area

Sediment concentrations were estimated by measuring the amount of sediment in snow samples taken with a corer from the snow glide depositions in spring 2013 (Fig. 2). The corer allowed for the sampling of the entire depth of the snow deposition and thus the integration of the sediment yield over the depth of the deposition. For larger depositions, samples were collected along two transects across each deposition. For smaller depositions, we took three samples. The samples were melted and filtered through a 0.11 µm filter. The filtered material was dried at 40 °C and weighted to obtain the concentration of sediment per sample (M_s). The mean sediment values (and for depositions with several samples the interpolated mean sediment values) were used to estimate the total sediment load of the snow glide deposition (M_A) according to

$$M_A = \frac{A_A \times M_s}{A_c}, \qquad (1)$$

where A_c is the area of the corer and A_A is the area of the snow glide deposition. The latter was mapped in the field by GPS and measuring tape. Sediment load was further converted to soil erosion rate (E) by

$$E = \frac{M_\mathrm{A}}{A_\mathrm{s}}, \tag{2}$$

where A_s is the source area of the snow and sediment deposition. Each snow glide was photo-documented and the respective source area was mapped with GPS and transferred to ArcGIS for surface area estimation.

2.3.2 Assessment of soil redistribution by water erosion using the RUSLE

The USLE (Wischmeier and Smith, 1978) and its revised version the RUSLE (Renard et al., 1997) are empirical erosion models originally developed in the US. Several adapted versions for other regions as well as for different temporal resolutions have been developed and applied more or less successfully (Kinnell, 2010). Despite its well-known limitation (highlighted in our introduction), we selected RUSLE because of the lack of simple soil erosion models specific for mountain areas and, moreover, because of its better performance when compared to the other existing models (Konz et al., 2010; Meusburger et al., 2010b). The RUSLE can be calculated using the following equation:

$$A = R \times K \times \mathrm{LS} \times C \times P, \tag{3}$$

where A is the predicted average annual soil loss ($\mathrm{t\,ha^{-1}\,yr^{-1}}$). R is the rainfall–runoff-erosivity factor ($\mathrm{N\,h^{-1}}$) that quantifies the effect of raindrop impact and reflects the rate of runoff likely to be associated with the rain (Renard et al., 1997). The soil erodibility factor K ($\mathrm{kg\,h\,N^{-1}\,m^{-2}}$) reflects the ease of soil detachment by splash or surface flow. The parameter LS (dimensionless) accounts for the effect of slope length (L) and slope gradient (S) on soil loss. The C factor is the cover factor, which represents the effects of all interrelated cover and management variables (Renard et al., 1997).

For comparability between the RUSLE estimates of Konz et al. (2009) and the ones assessed in this study, we used the same R factor approximation of Rogler and Schwertmann (1981) adapted by Schuepp (1975). According to the USLE procedure, snowmelt can be integrated into erosivity calculation by multiplying snow precipitation by 1.5 and then adding the product to the kinetic energy times the maximum 30 min intensity. However, the latter procedure does not account for redistribution of snow by drifting, sublimation and reduced sediment concentrations in snowmelt (Renard et al., 1997). Therefore, as suggested by Renard et al. (1997), this adaption of the R factor was not considered in this study. The K factor was calculated with the K nomograph after Wischmeier and Smith (1978), using grain size analyses and the carbon contents of the upper 15 cm of the soil profiles. Total C content of soils was measured with a Leco CHN analyser 1000, and grain size analyses were performed with sieves for grain sizes between 32 and 1000 µm and with a Sedigraph 5100 (Micromeritics) for grain sizes between 1 and 32 µm. L and S were calculated according to Renard et al. (1997). The support-and-practice factor P (dimensionless) was set to 0.9 for some of the pasture sites because alpine pastures with cattle trails resemble small terrace structures, which, it is suggested, are considered in P (Foster and Highfill, 1983). For all other sites, the value of P was set to 1. The cover-and-management factor C was assessed separately for sites with and without dwarf shrubs using measured fractional vegetation cover (FVC) in the field.

For investigated sites without dwarf shrubs (US Department of Agriculture, 1977), the C factor can be estimated with

$$C = 0.45 \times e^{-0.0456 \times \mathrm{FVC}}, \tag{4}$$

and for sites with dwarf shrubs, the following equation was used:

$$C = 0.45 \times e^{-0.0324 \times \mathrm{FVC}}. \tag{5}$$

The FVC was determined in April and September using a grid of 1 $\mathrm{m^2}$ with a mesh width of 0.1 $\mathrm{m^2}$. The visual estimate of each mesh was averaged for the entire square metre. This procedure was repeated four times for each plot. The maximum standard deviation was approximately 5 %. For the *Alnus viridis* sites, we used the value provided by the US Department of Agriculture (1977), i.e. 0.003. This value assumes a fall height of 0.5 m and a ground cover of 95–100 %.

The uncertainty assessment of the RUSLE estimates is based on the measurement error of the plot steepness (±2 %), which was determined by repeated measurements and slope length (±12.5 m). An error of ±2 % was assumed for the grain size analyses as well as for the organic carbon determination. These errors were propagated through the K factor calculation. An error of ±20 % based on the observed variability between spring and autumn of FVC on the plots was used for the determination of the C factor. For the R factor an error of ±5 $\mathrm{N\,h^{-1}}$, which corresponds to the observed variability between the sites, was assumed. Finally, error propagation for the multiplication of the single RUSLE factors was done.

2.3.3 ^{137}Cs to assess total net soil redistribution

A 2 × 2 inch NaI-scintillation detector (Sarad, Dresden, Germany) was used to measure the in situ ^{137}Cs activity. The detector was mounted perpendicular to the ground at a height of 25 cm to reduce the radius of the investigated area to 1 m. Measurement time was set at 3600 s, and each site was measured three times.

The detector was successfully ($R^2 = 0.86$) calibrated against gamma spectroscopy laboratory measurements with a

20 % relative efficiency Li-drifted Ge detector (GeLi; Princeton Gamma-Tech, Princeton, NJ, USA) at the Department for Physics and Astronomy, University of Basel. For the GeLi detector, the resulting measurement uncertainty concerning the ^{137}Cs peak area (at 662 keV) was lower than 8 % (error of the measurement at 1σ) (Schaub et al., 2010). Gamma spectrometry calibration and quality control of the analysis were performed following the protocol proposed by Shakhashiro and Mabit (2009).

Soil moisture influences the measured ^{137}Cs activity. Thus, soil moisture measurements with an EC-5 sensor (DecagonDevices) were used to correct the in situ measurements. The NaI detector has the advantage of providing an integrated measurement over an area of 1 m^2. The commonly observed, intrinsic small-scale variability ($\sim$ 30 %) for ^{137}Cs (Sutherland, 1996; Kirchner, 2013) is thus smoothed. Nonetheless, around 10 % of the uncertainty of the ^{137}Cs-based soil erosion values can be attributed to the variability of replicated measurements on each single plot. The main error of the in situ measurement results from the peak area evaluation and was determined to be 17 % (Schaub et al., 2010).

With the ^{137}Cs method, soil redistribution rates are calculated by comparing the isotope inventory for an eroding point with a local reference inventory where neither erosion nor soil accumulation is expected. In the Ursern Valley, the initial reference ^{137}Cs fallout originated from thermonuclear weapon tests in the 1950s–1960s and the nuclear power plant accident of Chernobyl in 1986.

For the conversion of the ^{137}Cs inventories to soil erosion rates, knowledge about the proportion of Chernobyl ^{137}Cs fallout is a key parameter for the estimation of erosion rates; however, only few data are available. Pre-Chernobyl (1986) ^{137}Cs activities of the top soil layers (0–5 cm) of between 2 and 58 Bq kg^{-1} (one outlier of 188 Bq kg^{-1} in Ticino) were recorded for 12 sites distributed across Switzerland (Riesen et al., 1999). After radioactive decay, in 2007, only 1–35 Bq kg^{-1} are left. The ^{137}Cs activity for the flat reference sites near the valley bottom (1469–1616 m a.s.l) was estimated as 146 ± 20 Bq kg^{-1} (Schaub et al., 2010). The investigated sites are located in close vicinity to the reference sites and at a comparable altitude (1476–1670 m a.s.l). Consequently, the maximum contribution of pre-Chernobyl ^{137}Cs might represent 20 % at reference sites.

Additionally, vertical migration must be considered. In literature migration values between 0.03 and 1.30 cm yr^{-1} are reported (Schimmack et al., 1989; Arapis and Karandinos, 2004; Schuller et al., 2004; Schimmack and Schultz, 2006; Ajayi et al., 2007). In the Ursern Valley, ^{137}Cs activity (Bq kg^{-1}) declines exponentially with soil depth. Therefore, for the conversion of ^{137}Cs measurements to soil erosion rates, the well-known profile distribution model (Walling et al., 2011) was adapted for direct use with the ^{137}Cs activity profile (Konz et al., 2009, 2012). We set the particle size factor to 1 because no preferential transport of the finer soil particles was observed for our sites (Konz et al., 2012). In contrast, no preferential transport or preferential transport of coarse material occurred, most likely due to snow- and animal-induced particle transport (see Konz et al., 2012). The calculation of the erosion rates refers to the period 1986–2007 because, pre-Chernobyl, ^{137}Cs is negligible. For uncultivated sites the diffusion and migration model is an alternative to the profile distribution model. However, the ^{137}Cs depth profile at our reference sites did not follow a polynomial distribution and thus did not allow for a successful fit of the diffusion and migration coefficient. Due to the integrative and repeated measurement with the NaI detector, the errors associated with measurement precision are assumed to be largely cancelled out. However, the error associated with the spatial variability of the reference inventory ($\pm$20 Bq kg^{-1}) was propagated through the conversion model in order to receive an upper and lower confidence interval for the resulting erosion estimates.

2.4 Spatial modelling of snow glide distances

We used the spatial snow glide model (SSGM; Leitinger et al., 2008) to predict potential snow glide distances for an area of approximately 30 km^2 surrounding our study sites. The SSGM is an experimental model, which includes the following parameters: the forest stand, the slope angle, winter precipitation, the slope and the static friction coefficient μ_s ($-$). Slope angle and slope aspect were derived from a high-precision digital elevation model (DEM) with 2 m resolution and an accuracy of $\pm$0.5 m at 1σ in open terrain and $\pm$1.5 m at 1σ in terrain with vegetation. Above 2000 m a.s.l., a DEM with 25 m resolution and an average error of 1.5 m for the Central Plateau and the Jura, 2 m for the Prealps and the Ticino and 3 to 8 m for the Alps was used (Swisstopo). Winter precipitation was derived from the MeteoSwiss station located in Andermatt. We used the result from a QuickBird land cover classification with a resolution of 2.4 m (subsequently resampled to 5 m) as land cover input (Meusburger et al., 2010a). Combining this land cover map with a land use map (Meusburger and Alewell, 2009), it was possible to derive the parameter forest stand. A uniform static friction coefficient (μ_s) was assigned to each of the four investigated land cover types.

The static friction coefficient can be derived by

$$\mu_s = \frac{F_r}{F_n}, \tag{6}$$

where F_n (g m s^{-2}) is the normal force that can be calculated with

$$F_n = m \times g \times \cos\alpha, \tag{7}$$

where g is the standard gravity (9.81 m s^{-2}), α is the slope angle (°) and m is the weight of the snow glide shoe (in our study 202 g).

The initial force (F_r; with the unit g m s^{-2}) which is needed to get the glide shoe moving on the vegetation surface was measured with a spring balance (Pesola® Medio 1000 g) and multiplied with the standard gravity. To obtain representative values of F_r the measurement was replicated 10 times per sample site and subsequently averaged. The parameter estimates the surface roughness, induced by different vegetation types and land uses. A detailed description of the model and its parameters has been provided by Leitinger et al. (2008).

Supplemented by snow glide measurements from this study, the SSGM (i.e. ordinary least squares, OLS, regression equation) was refined to be valid also for north-facing sites and sites with *Alnus viridis*. Consequently, the revised SSGM is given by the equation

$$\ln(\hat{y}) = 0.337 - 0.925x_1 + 0.095x_2 + 0.01x_3 + 1.006x_4 + 0.839x_5 + 0.076x_6 - 0.075x_7^2, \quad (8)$$

where $\hat{y}$ is the estimated snow-gliding distance (mm), x_1 is the forest stand (0; 1), x_2 is the slope angle (°), x_3 is the winter precipitation (mm), x_4 is the eastern slope aspect (0; 1), x_5 is the souther slope aspect (0; 1), x_6 is the western slope aspect (0; 1) and x_7 is the static friction coefficient. The revised SSGM was highly significant ($p < 0.001$), with a determination coefficient of 0.581 (adjusted R^2).

The model was then applied for the winter period of 2009/2010 (285 mm winter precipitation) and for the long-term average winter precipitation (430 mm winter precipitation for the years 1959 to 2010).

3 Results and discussion

3.1 Snow glide measurements 2009/2010

For each site, the static friction coefficient, as a measure of surface roughness, was determined in autumn prior to the installation of the snow glide shoes. Lowest surface roughness was observed for the hayfields, followed by soil surface at sites covered with *Alnus viridis* on the north-facing slope (Table 1). For the pastures without dwarf shrubs, the two mean monitored values differed ($\mu_s = 0.37$ and 0.68) but were similar to those of pastures with dwarf shrubs ($\mu_s = 0.66$ to 0.69). Slightly higher values were observed for the dense undergrowth of *Alnus viridis* sites on the south-facing slope ($\mu_s = 0.70$ and 0.84). These static friction coefficients are within the range of 0.22–1.18 reported by Leitinger et al. (2008).

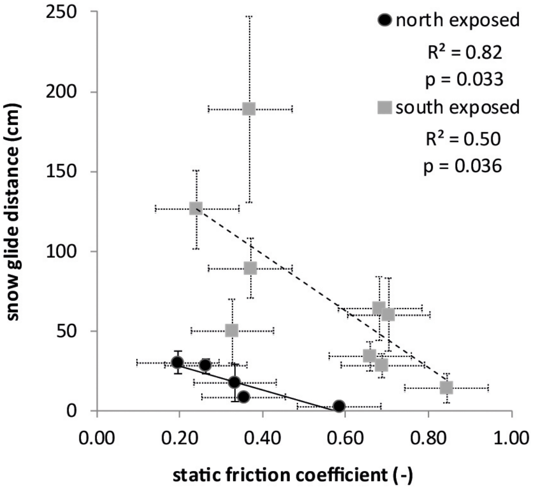

Figure 3. Snow glide distance against the static friction coefficient for the south- and north-facing slope sites (represented by squares and dots, respectivey). *Y* error bars represent the standard deviation of replicate measurements at one site. For the static friction coefficient, an error of ±0.1 (corresponding to the scale accuracy of the spring balance) was assumed.

The snow glide measurements confirmed the presence and the potential impact of this process in our investigated sites. The mean measured snow glide distances (sgd) of the different sites varied from 2 to 189 cm (see Table 1). The main part of this variability can be explained by the slope aspect and the surface roughness (see Fig. 3). With increasing surface roughness (expressed as the static friction coefficient, μ_s) the snow glide distance declines. This decrease is more pronounced for the south-facing slope (sgd $= -1547.2\,\mu_s + 172.93$; $R^2 = 0.50$; $p = 0.036$). For the north-facing slope, the snow glide distances and the variability are lower. Approximately 80 % of the observed variability on the north-facing slope can be explained by the surface roughness (sgd $= -622.17\,\mu_s + 43.09$; $R^2 = 0.82$; $p = 0.033$). The identification of slope aspect and surface roughness as main causal factors for snow gliding corresponds to the findings of other studies (In der Gand and Zupancic, 1966; Newesely et al., 2000; Hoeller et al., 2009). According to several studies on the seasonal snow–soil interface conditions (In der Gand and Zupancic, 1966; McClung and Clarke, 1987; Leitinger et al., 2008), snow gliding on south-facing sites is preferential in spring, when high solar radiation leads to a high proportion of melting water at the soil–snow interface. However, in autumn, snow gliding primarily occurs when a huge amount of snow falls on the warm soil. In this case, north-facing sites may be confronted with high snow gliding activity as well.

Our measured snow glide distances are comparable to those recorded by other researchers. For example, during a 7-year period in the Austrian Alps, Höller et al. (2009) monitored a snow glide distance of 10 cm within the forest, 170 cm in cleared forest sites and up to 320 cm for open fields. Margreth (2007) found total glide distances of 19 to 102 cm for an 11-year observation period in the Swiss Eastern Alps (south-east facing slope at 1540 m a.s.l.).

3.2 Soil erosion estimates

Snow glide depositions were observed for seven sites; for one site a wet avalanche deposition (pN) and for four sites

Table 1. Parameters related to measured snow glide distance (sgd; SD is the standard deviation based on three to five replicate measurements) for the investigation sites in the Ursern Valley, Switzerland. N indicates the sites on the north-facing slope.

Site	Vegetation	Slope (°)	Initial force Fr ($\mathrm{g\,m\,s^{-2}}$)	Static friction coefficient µs (–)	Measured sgd (cm)	SD sgd (cm)
h1	hayfield	39	569	0.37	189	117
h2	hayfield	38	510	0.33	50	40
h3	hayfield	35	392	0.24	126	49
pw1	pasture with dwarf shrubs	38	1030	0.66	34	19
pw2	pasture with dwarf shrubs	35	1118	0.69	28	15
p1	pasture	38	579	0.37	89	37
p2	pasture	35	1109	0.68	64	40
h1N	hayfield	28	343	0.20	30	14
h2N	hayfield	30	608	0.35	8	1
pN	pasture	18	628	0.33	17	23
A1N	*Alnus viridis*	25	1050	0.58	2	1
A2N	*Alnus viridis*	30	451	0.26	28	9
A1	*Alnus viridis*	22	1550	0.84	14	18
A2	*Alnus viridis*	31	1197	0.70	60	46

no snow glide depositions were observed (Table 3). The four sites without snow glide depositions were all located on the north-facing slope. The erosion rates estimated from the sediment yields of the snow glide deposition ranged from 0.03 to 22.9 $\mathrm{t\,ha^{-1}\,yr^{-1}}$. The maximum value was determined for the site h1 which is in agreement with the ^{137}Cs method. For sites with snow glide depositions, a mean value of 8.4 $\mathrm{t\,ha^{-1}\,yr^{-1}}$ was measured. The somewhat high erosion rates are documented in a photo from the spring (Fig. 4). The winter 2012/2013 precipitation of 407 mm was quite representative of the long-term average (i.e. 430 mm). On average, the pastured sites without dwarf shrubs produced the highest measured sediment yields, followed by the hayfields, and considerably lower values were observed for the pastures with dwarf shrub sites. Whether the observed difference is due to the different vegetation cover or due to site-specific topography cannot be solved conclusively with the present data set. A wet avalanche was observed for the site pN. Interestingly, at 1.97 $\mathrm{t\,ha^{-1}\,yr^{-1}}$, the estimated erosion rate of the wet avalanche deposition was smaller than most of the snow-gliding-related erosion rates. However, high erosion rates of 3.7 and 20.8 $\mathrm{t\,ha^{-1}}$ per winter due to wet avalanches have been reported at a study site located in the Aosta Valley, Italy (Ceaglio et al., 2012). At this study site, where the major soil loss is triggered by wet avalanches, the snow-related soil erosion estimated from the deposition area was comparable to the yearly total erosion rates assessed with the ^{137}Cs method (13.4 and 8.8 $\mathrm{t\,ha^{-1}\,yr^{-1}}$; Ceaglio et al., 2012).

On the north-facing slope, an average RUSLE estimate of 1.8 $\mathrm{t\,ha^{-1}\,yr^{-1}}$ with a maximum value of 3.8 $\mathrm{t\,ha^{-1}\,yr^{-1}}$ was established (Table 2). The, on average, lower values as compared to the south-facing slope (6.7 $\mathrm{t\,ha^{-1}\,yr^{-1}}$) are due to lower slope angles (thus lower LS factor values) and C factors (due to a higher fractional vegetation cover). This effect was not compensated for by the, on average, higher K factor of 0.40 $\mathrm{kg\,h\,N^{-1}\,m^{-2}}$ on the north-facing slopes. The higher K factor is caused by a 6 % higher proportion of very fine sand. The mean RUSLE-based soil erosion rate for all sites was 4.6 $\mathrm{t\,ha^{-1}\,yr^{-1}}$.

Figure 4. Example of snow glide deposits for the site p1.

The mean ^{137}Cs-based soil erosion rate of 17.8 $\mathrm{t\,ha^{-1}\,yr^{-1}}$ is approximately 4 times as high as the average RUSLE estimates. Congruent with RUSLE, the ^{137}Cs-based average soil erosion rate on the north-facing slopes is lower than on the south-facing slopes (by 8.7 $\mathrm{t\,ha^{-1}\,yr^{-1}}$). The highest ^{137}Cs-based soil erosion estimates are found at two hayfield sites (h1 and h3) and the pasture sites on the south-facing slope (p1 and p2). The higher RUSLE and ^{137}Cs estimates on the more intensely used, steeper and more

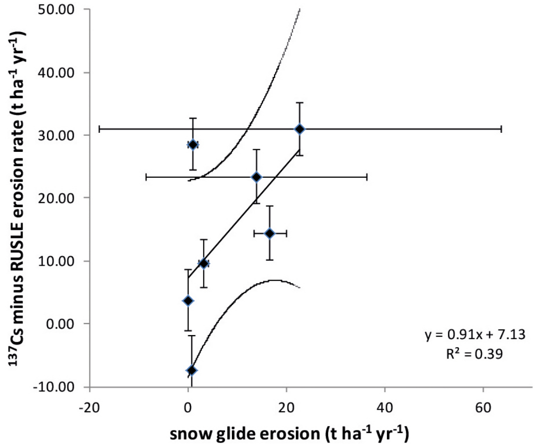

Figure 5. Snow glide erosion estimated from the snow glide deposit sediment yield against the difference of the ^{137}Cs and RUSLE soil erosion rate (t ha^{-1} yr^{-1}). Y error bars represent the uncertainty of both the ^{137}Cs and RUSLE estimates. X error bars represent the standard deviation of erosion rates resulting from several sediment measurements within one snow glide deposit. The solid line represents the obtained linear regression and the dotted lines the 95 % confidence interval.

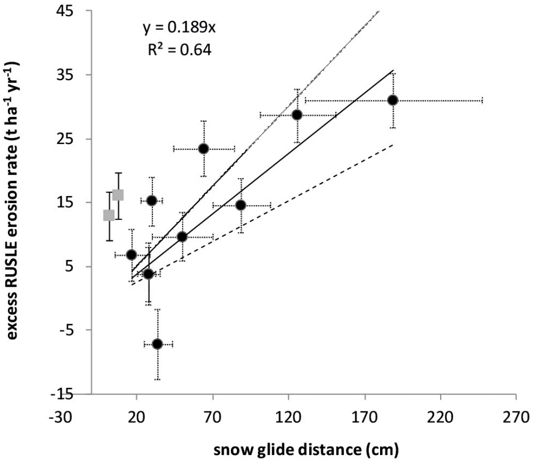

Figure 6. Correlation of the cumulative snow glide distances (cm) measured for the winter of 2009/2010 versus the difference of the ^{137}Cs and RUSLE soil erosion rate (t ha^{-1} yr^{-1}) for the grassland sites (dots, $n = 10$) and the *Alnus viridis* sites (A1N, A2N; squares, $n = 2$). Y error bars represent the error of both the ^{137}Cs and RUSLE estimates. X error bars represent the standard deviation of replicate snow glide measurements at one site. Solid line represents a linear regression and the dotted lines the 95 % confidence interval.

snow-glide-affected south-facing slope are reasonable. However, the high ^{137}Cs-based erosion rates (16.6 t ha^{-1} yr^{-1} for A1N and 13.7 t ha^{-1} yr^{-1} for A2N) at *Alnus viridis* sites are unexpected and will be discussed below.

3.3 Relation between soil redistribution and snow gliding

Sediment yield measurements in snow glide depositions showed the importance of this process in the winter of 2012/2013. However, even though the winter was quite representative of the average winter conditions (in terms of winter precipitation), the measured rates are likely to vary between different years. To assess the relevance of this process for a longer timescale, a second approach using RUSLE and ^{137}Cs was followed.

Our hypothesis was that the difference of the water soil erosion rate modelled with RUSLE and the total net erosion measured with the ^{137}Cs method correlates to a "winter soil erosion rate". This winter soil erosion rate comprises long-term soil removal by snow gliding and occasionally wet avalanches as well as snowmelt. These "winter erosion rates" (difference of ^{137}Cs and RUSLE) ranged from rates of −7.3 t ha^{-1} yr^{-1} for a pasture with dwarf shrubs to rates of 31 t ha^{-1} yr^{-1} for the hayfield site h1. According to our hypothesis, a negative difference of ^{137}Cs and RUSLE indicates a sedimentation (because RUSLE simulates the potential water soil erosion rates) and a positive value indicates erosion due to processes not implemented in the RUSLE. The most likely processes would be snow-induced processes. Two observations underpin our hypothesis: first, even though the sediment yield measurements in the snow glide deposition comprise only one winter, a relation ($p = 0.13$) between the snow glide erosion and the difference of ^{137}Cs and RUSLE could be observed ($R^2 = 0.39$; Fig. 5). The largest difference between ^{137}Cs- and RUSLE-based erosion could be observed for sites with high snow-glide-related sediment yield (except for the site h3). The resulting intercept might be either due to a deviation of the weather conditions in the winter of 2012/2013 from the long-term average condition captured by the other methods or due to the impact of occasional wet avalanches and/or snowmelt. For instance, following the USLE snowmelt adaptation for the R factor would result in an, on average, 2.1 t ha^{-1} yr^{-1} higher modelled erosion rate for all sites.

A further indication for the importance of snow gliding as a soil erosion agent is given by the significant positive correlation between measured snow glide distance and the difference of ^{137}Cs and RUSLE, which we interpret as the winter soil erosion rate (Fig. 6). The measured snow glide distance explained 64 % of the variability of the winter soil erosion rate ($p < 0.005$). However, this relation does not comprise the *Alnus viridis* sites that showed a large difference between RUSLE- and ^{137}Cs-based rates but a short snow glide distance. For the *Alnus viridis* sites, we have to expect that either one of the two approaches to determine soil erosion rates is erroneous and/or that we have another predominant erosion process not considered or not correctly parameterised in the RUSLE yet. A possible error related to the ^{137}Cs approach might be that ^{137}Cs was intercepted by leaf and litter

Table 2. Measured site characteristics (SOC stands for soil organic carbon; vfs stands for very fine sand fraction), resulting RUSLE factors and soil erosion rates and ^{137}Cs-based erosion rates for the investigation sites in the Ursern Valley, Switzerland. * indicates the sites from Konz et al. (2009).

Site	Slope (°)	SOC (%)	vfs (%)	Silt (%)	Clay (%)	K factor (kg h N^{-1} m^{-2})	P factor (–)	LS factor (–)	R factor (N h^{-1})	C factor (–)	RUSLE (t ha^{-1} yr^{-1})	^{137}Cs (t ha^{-1} yr^{-1})
h1*	39	7.7	12.9	47.3	12.5	0.280	1.00	22.2	97.2	0.010	6.0	37.0
h2*	38	7.2	9.7	58.8	17.3	0.290	1.00	8.8	94.5	0.006	1.5	11.0
h3*	35	7.4	12.3	43.8	16.9	0.230	1.00	20.7	93.6	0.010	4.5	33.0
pw1*	38	6.9	6.3	63.5	10.8	0.320	0.90	12.6	91.7	0.040	13.3	6.0
pw2*	35	7.1	11.2	40.9	14.2	0.230	0.90	11.8	94.8	0.040	9.3	13.0
p1*	38	7.6	11.2	50.5	11.6	0.270	0.90	11.8	97.6	0.020	5.6	20.0
p2*	35	7.2	12.4	45.6	15.0	0.250	0.90	15.3	96.4	0.020	6.6	30.0
h1N	28	4.8	18.5	41.0	5.8	0.416	1.00	7.0	93.6	0.012	3.2	18.3
h2N	30	4.3	13.7	48.0	8.5	0.419	1.00	8.4	91.7	0.012	3.8	7.5
pN	18	6.2	17.5	38.7	10.2	0.369	1.00	1.1	97.2	0.012	0.5	7.2
A1N	25	3.8	16.1	43.8	9.7	0.399	1.00	5.3	93.6	0.003	0.6	16.6
A2N	30	6.8	18.7	39.7	9.6	0.389	1.00	8.4	91.7	0.003	0.9	13.7
Mean of north-facing sites	37	7.3	10.9	50.1	14.0	0.267	0.94	14.7	95.1	0.021	6.7	21.4
Mean of south-facing sites	26	5.2	16.9	42.2	8.8	0.398	1.00	6.0	93.6	0.008	1.8	12.7
Mean of all sites	32.4	6.4	13.4	46.8	11.8	0.3	1.0	11.1	94.5	0.0	4.6	17.8

Table 3. Snow-movement-related soil erosion derived from the difference of ^{137}Cs-based and RUSLE-based erosion rates (Diff.) and from field measured sediment in snow glide deposits (sg erosion). For each snow glide deposit, the mean sediment yield estimate is based on several samples (n). SD is the standard deviation for the resulting erosion rates based on the individual sediment yield samples and * indicates the sediment yield of a wet avalanche. "Uncertainty Diff." provides the uncertainty of Diff. resulting from both the ^{137}Cs and RUSLE method.

Site	RUSLE (t ha^{-1} yr^{-1})	^{137}Cs (t ha^{-1} yr^{-1})	Diff. ^{137}Cs−RUSLE (t ha^{-1} yr^{-1})	Uncertainty Diff. (t ha^{-1} yr^{-1})	sg erosion (t ha^{-1} yr^{-1})	SD sg erosion (t ha^{-1} yr^{-1})	n
h1	6.0	37.0	31.0	8.5	22.9	81.5	16
h2	1.5	11.0	9.5	7.7	3.2	1.9	3
h3	4.5	33.0	28.5	8.2	1.1	1.9	10
pw1	13.3	6.0	−7.3	10.9	0.8	0.5	3
pw2	9.3	13.0	3.7	9.8	0.0	0.1	7
p1	5.6	20.0	14.4	8.5	16.7	6.8	11
p2	6.6	30.0	23.4	8.6	14.0	44.9	13
h1N	3.2	18.3	15.1	7.6	nosnow glide	–	–
h2N	3.8	7.5	3.7	8.4	no snow glide	–	–
pN	0.5	7.2	6.7	8.0	1.97*	3.8	18
A1N	0.6	16.6	16.0	7.2	no snow glide	–	–
A2N	0.9	13.7	12.8	7.6	no snow glide	–	–

material of *Alnus viridis*. Thus, a reference site with *Alnus viridis* stocking would be necessary which is difficult to find at our site because no flat areas exist with *Alnus viridis* stocking. The observation of increasing soil erosion with an increasing snow glide rates is congruent with the findings of Leitinger et al. (2008), who observed that the severity of erosion attributed to snow gliding (e.g. torn-out trees, extensive areas of bare soil due to snow abrasion, landslides in topsoil) was high in areas with a high snow glide distance and vice versa.

Generally, for these subalpine sites the magnitude of the RUSLE-based water erosion rates needs to be considered with caution not only with respect to the uncertainties involved but also conceptually since several of the factors lay outside the empirical RUSLE framework. Also, the magnitude of the ^{137}Cs-based erosion rate needs to be considered carefully. The profile distribution model tends to overestimate soil erosion rates since it assumes that the ^{137}Cs depth distribution does not change with time. However, in the very first years after the fallout, ^{137}Cs was concentrated more in the surface soil layer (Schimmack and Schultz, 2006). Thus, in the years after the fallout, small losses of soil would have resulted in a relatively high ^{137}Cs loss which might result in an overestimation of soil erosion rates.

The latter uncertainties do not include snowmelt erosion and temporal variability, both potential reasons for the intercept observed between the magnitude of winter erosion estimated from RUSLE/^{137}Cs and from snow glide depositions. Nonetheless, the almost 1 : 1 relation is a clear indication that the observed discrepancies between the RUSLE- and

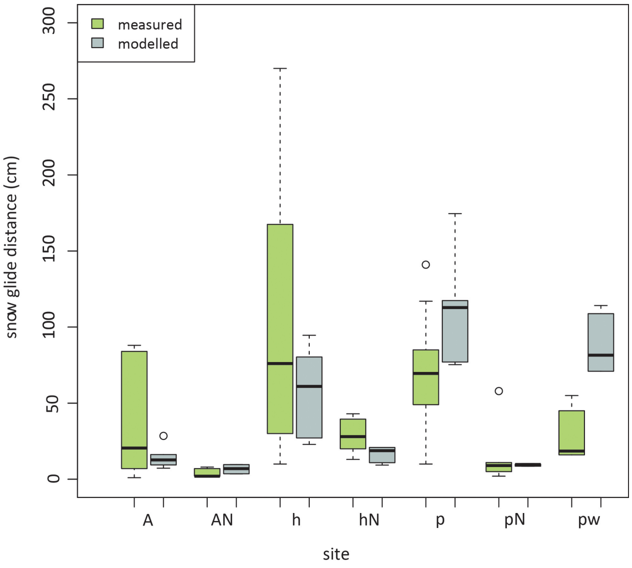

Figure 7. Box plot of measured snow glide distances and corresponding modelling results for different land use/land cover types (hayfields – h; pastures – p; pastures with dwarf shrubs – pw; and abandoned grassland covered with *Alnus viridis* – A) for the winter period of 2009/2010. N indicates the sites on the north-facing slope.

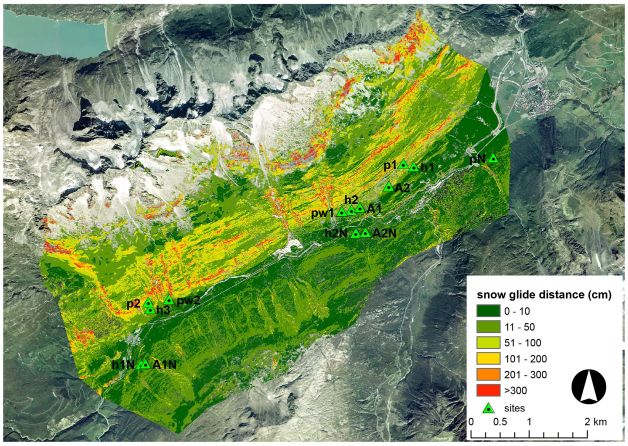

Figure 8. Map of the potential snow glide distance (m) modelled by SSGM.

^{137}Cs-based soil erosion rates are related to snow gliding. Congruent with our results, Stanchi et al. (2014) found a relation between the intensity of snow-erosion-affected areas and the difference of RUSLE and ^{137}Cs estimates.

Further, it can be deduced that low surface roughness is correlated to high snow glide distances, and these are, in turn, positively correlated to large observed differences between RUSLE- and ^{137}Cs-based soil erosion rates that we interpret as high winter soil erosion rates. Erosion estimates from sediment yield measurements of the snow glide deposition could confirm the partially high winter erosion rates. However, the presented relations might be highly variable, depending on soil temperature (whether the soil is frozen or not) during snow, the occurrence of a water film that allows a transition of dry to wet gliding (Haefeli, 1948) and on the weather conditions of a specific winter. In addition, some of the investigated sites might also be affected by avalanches in other years.

3.4 Modelled snow glide distances

The modelled snow glide rates from the SSGM compared reasonably well with the snow glide measurements (Fig. 7). In agreement with the measured values, all sites facing to the north revealed lower modelled snow glide distances. Largest discrepancies between the mean modelled and measured values of each site occur for the pastures on the south-facing slopes (p and pw). The model overestimates the snow glide rates for these sites, which might be due to the effect of microrelief in form of cattle trails at these sites. These small terraces (0.5 m in width) most likely reduce snow gliding but are not captured by the digital elevation model that is used for the SSGM. In general, modelled snow glide distances show smaller ranges than measured snow glide distances, due to the 5 m resolution of the model input data (Fig. 7). Interestingly, the occurrence of dwarf shrubs seems to reduce snow gliding to a larger extent than predicted by the model.

The modelled snow glide distance map (Fig. 8) is based on the long-term average of winter precipitation, which, at 430 mm, is clearly higher than the winter precipitation in 2009/2010 (at 285 mm; Fig. 7). The highest snow glide values were simulated on the steep, south-facing slopes with predominately grassland and dwarf-shrub cover. Very high rates are also found on the lower parts of the south-facing slopes that are used as pastures and hayfields. The smallest snow glide rates are located on the north-facing slopes. The map clearly reproduces the effect of topography and aspect. Moreover, snow glide distances summarised for predominant land use types also reproduce the impact of vegetation cover (Fig. 9). The highest potential snow glide distances were simulated by the SSGM for the south-facing hayfield and pasture sites, while the *Alnus viridis* has, on average, decidedly smaller snow glide distances. In contrast, on the north-facing slopes, there is no difference observed between the *Alnus viridis* and the hayfield category. Here the pasture sites show the highest average snow glide rate. The interpretation of the differences between land use types is, however, restricted since systematically different topographic conditions are involved.

The topographic and climatic conditions in our valley resemble the environment under which the SSGM was initially developed; nonetheless, further regular yearly measurement would be needed to improve the performance of the model in this area. In conclusion, the application of the SSGM highlighted the relevance of the snow gliding process and the potentially related soil erosion for (sub-) alpine areas.

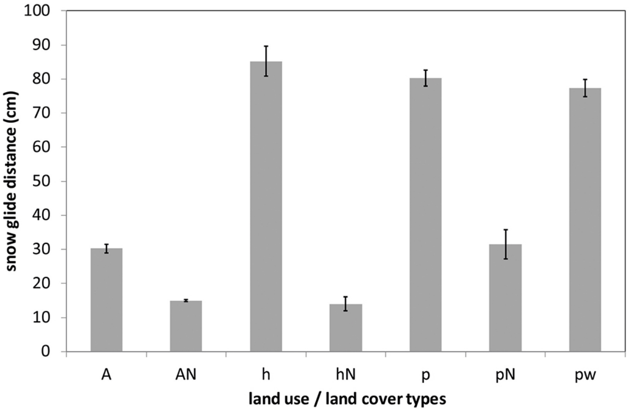

Figure 9. Modelled potential snow glide distances (using long-term average winter precipitation) as mean for the whole catchment grouped by predominant land use/land cover types (hayfields – h; pastures – p; pastures with dwarf shrubs – pw; *Alnus viridis* sites – A). N indicates the sites on the north-facing slope. Error bars indicate the standard error of the mean.

4 Conclusions

The presented absolute magnitude of the snow-glide-related soil erosion rate is subject to high interannual variability. However, snow glide erosion measured from the snow glide depositions (0.03 to 22.9 $\mathrm{t\,ha^{-1}\,yr^{-1}}$ in the winter of 2012/2013) highlights the need to consider the process of snow gliding as a soil erosion agent in steep, scarcely vegetated alpine areas.

RUSLE and ^{137}Cs both yield average long-term soil erosion rates for water and total net erosion, respectively. Despite the associated uncertainties, the total net erosion rate is significantly higher than the gross water erosion rate provided by RUSLE. We interpret the difference as a “winter” soil erosion rate which was significantly correlated to snow glide rates and showed an almost 1 : 1 relation to sediment yield measurements in snow glide depositions. The application of RUSLE and ^{137}Cs showed (i) the relevance of the snow glide process for a longer timescale (as compared to the snow glide deposition measurements of one winter) and (ii) that, for an accurate soil erosion prediction in high mountain areas, it is crucial to assess and quantify the erosivity of snow movements.

The spatial snow glide model might serve as a tool to evaluate the spatial relevance of snow gliding for larger areas. However, it is recommended to additionally estimate the kinetic energy that acts upon the soil during the snow movement. This would allow for a direct comparison of rainfall erosivity and snow movement erosivity and, moreover, its insertion into soil erosion risk models. The impact of snow movement on soil removal should, moreover, be evaluated in the context of predicted changes in snow cover, e.g. an increase in snow amounts for elevated ($>$ 2000 m a.s.l.) areas (Beniston, 2006).

Further, we demonstrated that surface roughness, which is determined by the vegetation type and land use, reduces snow glide rates, particularly on the, in general, more intensely used south-facing slopes. In turn, snow glide rates are related positively to increasing soil loss at grassland sites. This is an important result with respect to soil conservation strategy, since surface roughness can be modified and adapted through effective land use management.

Acknowledgements. This study was funded by the Swiss Federal Office for the Environment (Contract no. StoBo-Bio/810.3129.004/05/0X). We would like to thank the two anonymous reviewers for their constructive comments, which greatly helped to improve our manuscript. T. Bogaard is gratefully acknowledged for handling the review process.

Edited by: T. Bogaard

References

Ackroyd, P.: Erosion by snow avalanche and implications for geomorphic stability, Torlesse Range, New-Zealand, Arct. Alp. Res., 19, 65–70, doi:10.2307/1551001, 1987.

Ajayi, I. R., Fischer, H. W., Burak, A., Qwasmeh, A., and Tabot, B.: Concentration and vertical distribution of ^{137}Cs in the undisturbed soil of southwestern Nigeria, Health Phys., 92, 73–77, 2007.

Alewell, C., Meusburger, K., Juretzko, G., Mabit, L., and Ketterer, M.: Suitability of $^{239+240}$Pu as a tracer for soil erosion in alpine grasslands, Chemosphere, 103, 274–280, doi:10.1016/j.chemosphere.2013.12.016, 2014.

Arapis, G. D. and Karandinos, M. G.: Migration of ^{137}Cs in the soil of sloping semi-natural ecosystems in Northern Greece, J. Environ. Radioact., 77, 133–142, doi:10.1016/j.jenvrad.2004.03.004, 2004.

Bell, I., Gardner, J., and Descally, F.: An estimate of snow avalanche debris transport, Kaghan Valley, Himalaya, Pakistan, Arct. Alp. Res., 22, 317–321, doi:10.2307/1551594, 1990.

Beniston, M.: Mountain weather and climate: A general overview and a focus on climatic change in the Alps, Hydrobiologica, 562, 3–16, 2006.

Benmansour, M., Mabit, L., Nouira, A., Moussadek, R., Bouksirate, H., Duchemin, M., and Benkdad, A.: Assessment of soil erosion and deposition rates in a Moroccan agricultural field using fallout 137Cs and 210Pbex, J. Environ. Radioact., 115, 97–106, doi:10.1016/j.jenvrad.2012.07.013, 2013.

Ceaglio, E., Meusburger, K., Freppaz, M., Zanini, E., and Alewell, C.: Estimation of soil redistribution rates due to snow cover related processes in a mountainous area (Valle d’Aosta, NW Italy), Hydrol. Earth Syst. Sci., 16, 517–528, doi:10.5194/hess-16-517-2012, 2012.

Confortola, G., Maggioni, M., Freppaz, M., and Bocchiola, D.: Modelling soil removal from snow avalanches: A case study in the North-Western Italian Alps, Cold Reg. Sci. Technol., 70, 43–52, doi:10.1016/j.coldregions.2011.09.008, 2012.

Foster, G. R. and Highfill, R. E.: Effect of terraces on soil loss – USLE P-factor values for terraces, J. Soil Water Conserv., 38, 48–51, 1983.

Freppaz, M., Godone, D., Filippa, G., Maggioni, M., Lunardi, S., Williams, M. W., and Zanini, E.: Soil Erosion Caused by Snow Avalanches: a Case Study in the Aosta Valley (NW Italy), Arct. Antarct. Alp. Res., 42, 412–421, doi:10.1657/1938-4246-42.4.412, 2010.

Fuchs, S. and Keiler, M.: Variability of Natural Hazard Risk in the European Alps: Evidence from Damage Potential Exposed to Snow Avalanches, in: Disaster Mangement Handbook, edited by: Pinkowski, J., Crc Press-Taylor & Francis Group, Boca Raton, 267–279, 2008.

Gardner, J. S.: Observations on erosion by wet snow avalanches, Mount Rae area, Alberta, Canada, Arct. Alp. Res., 15, 271–274, doi:10.2307/1550929, 1983.

Haefeli, R.: Schnee, Lawinen, Firn und Gletscher, in: Ingenieur-Geologie, edited by: Bendel, L., Springer Vienna, Wien, 1948.

Heckmann, T., Wichmann, V., and Becht, M.: Sediment transport by avalanches in the Bavarian Alps revisited – a perspective on modelling, in: Geomorphology in Environmental Application:, edited by: Schmidt, K. H., Becht, M., Brunotte, E., Eitel, B., and Schrott, L., Zeitschrift Für Geomorphologie Supplement Series, Gebruder Borntraeger, Stuttgart, 11–25, 2005.

Hoeller, P., Fromm, R., and Leitinger, G.: Snow forces on forest plants due to creep and glide, Forest Ecol. Manage., 257, 546–552, doi:10.1016/j.foreco.2008.09.035, 2009.

In der Gand, H. R. and Zupancic, M.: Snow gliding and avalanches, IAHS-AISH Publ., 69, 230–242, 1966.

IUSS: World reference base for soil resources, Tech. Rep., FAO, 2006.

Jomelli, V. and Bertran, P.: Wet snow avalanche deposits in the French Alps: Structure and sedimentology, Geogr. Ann. Ser. A, 83, 15–28, doi:10.1111/j.0435-3676.2001.00141.x, 2001.

Juretzko, G.: Quantifizierung der Bodenerosion mit 137Cs und USLE in einem alpinen Hochtal (Val Piora, CH), Master, Environmental Sciences, Basel, 1–152, 2010.

Kinnell, P. I. A.: Why the universal soil loss equation and the revised version of it do not predict event erosion well, Hydrol. Process., 19, 851–854, doi:10.1002/hyp.5816, 2005.

Kinnell, P. I. A.: Event soil loss, runoff and the Universal Soil Loss Equation family of models: A review, J. Hydrol., 385, 384–397, doi:10.1016/j.jhydrol.2010.01.024, 2010.

Kirchner, G.: Establishing reference inventories of ^{137}Cs for soil erosion studies: Methodological aspects, Geoderma, 211, 107–115, doi:10.1016/j.geoderma.2013.07.011, 2013.

Konz, N., Schaub, M., Prasuhn, V., Bänninger, D., and Alewell, C.: Cesium-137-based erosion-rate determination of a steep mountainous region, J. Plant Nutr. Soil Sci., 172, 615–622, doi:10.1002/jpln.200800297, 2009.

Konz, N., Baenninger, D., Konz, M., Nearing, M., and Alewell, C.: Process identification of soil erosion in steep mountain regions, Hydrol. Earth Syst. Sci., 14, 675–686, doi:10.5194/hess-14-675-2010, 2010.

Konz, N., Prasuhn, V., and Alewell, C.: On the measurement of alpine soil erosion, Catena, 91, 63–71, doi:10.1016/j.catena.2011.09.010, 2012.

Leitinger, G., Holler, P., Tasser, E., Walde, J., and Tappeiner, U.: Development and validation of a spatial snow-glide model, Ecol. Modell., 211, 363–374, doi:10.1016/j.ecolmodel.2007.09.015, 2008.

Mabit, L. and Bernard, C.: Assessment of spatial distribution of fallout radionuclides through geostatistics concept, J. Environ. Radioact., 97, 206–219, doi:10.1016/j.jenvrad.2007.05.008, 2007.

Mabit, L., Bernard, C., Laverdiere, M. R., Wicherek, S., Garnier, J., and Mouchel, J. M.: Assessment of soil erosion in a small agricultural basin of the St. Lawrence River watershed, Hydrobiologia, 410, 263–268, 1999.

Mabit, L., Bernard, C., and Laverdiere, M. R.: Quantification of soil redistribution and sediment budget in a Canadian watershed from fallout caesium-137 (^{137}Cs) data, Can. J. Soil Sci., 82, 423–431, 2002.

Mabit, L., Benmansour, M., and Walling, D. E.: Comparative advantages and limitations of the fallout radionuclides ^{137}Cs, ^{210}Pb(ex) and ^{7}Be for assessing soil erosion and sedimentation, J. Environ. Radioact., 99, 1799–1807, doi:10.1016/j.jenvrad.2008.08.009, 2008.

Mabit, L., Meusburger, K., Fulajtar, E., and Alewell, C.: The usefulness of 137Cs as a tracer for soil erosion assessment: A critical reply to Parsons and Foster (2011), Earth-Sci. Rev., 137, 300–307, doi:10.1016/j.earscirev.2013.05.008, 2013.

Margreth, S.: Snow pressure on cableway masts: Analysis of damages and design approach, Cold Reg. Sci. Technol., 47, 4–15, doi:10.1016/j.coldregions.2006.08.020, 2007.

Matisoff, G. and Whiting, P. J.: Measuring Soil Erosion Rates Using Natural (Be-7, Pb-210) and Anthropogenic (^{137}Cs, ^{239}Pu, ^{240}Pu) Radionuclides, Handbook of Environmental Isotope Geochemistry, Vols. 1 and 2, edited by: Baskaran, M., Springer-Verlag Berlin, Berlin, 487–519, 2011.

McClung, D. M. and Clarke, G. K. C.: The effects of free-water on snow gliding, J. Geophys. Res.-Solid, 92, 6301–6309, 1987.

Merritt, W. S., Letcher, R. A., and Jakeman, A. J.: A review of erosion and sediment transport models, Environ. Modell. Softw., 18, 761–799, 2003.

Meusburger, K. and Alewell, C.: On the influence of temporal change on the validity of landslide susceptibility maps, Nat. Hazards Earth Syst. Sci., 9, 1495–1507, doi:10.5194/nhess-9-1495-2009, 2009.

Meusburger, K., Banninger, D., and Alewell, C.: Estimating vegetation parameter for soil erosion assessment in an alpine catchment by means of QuickBird imagery, Int. J. Appl. Earth Obs. Geoinf., 12, 201–207, doi:10.1016/j.jag.2010.02.009, 2010a.

Meusburger, K., Konz, N., Schaub, M., and Alewell, C.: Soil erosion modelled with USLE and PESERA using QuickBird derived vegetation parameters in an alpine catchment, Int. J. Appl. Earth Obs. Geoinf., 12, 208–215, doi:10.1016/j.jag.2010.02.004, 2010b.

Meusburger, K., Mabit, L., Park, J.-H., Sandor, T., and Alewell, C.: Combined use of stable isotopes and fallout radionuclides as soil erosion indicators in a forested mountain site, South Korea, Biogeosciences, 10, 5627–5638, doi:10.5194/bg-10-5627-2013, 2013.

Nearing, M., Foster, G., Lane, L., and Finkner, S.: A process-based soil erosion model for USDA – water erosion prediction project technology, Trans. Am. Soc. Agr. Eng., 32, 1587–1593, 1989.

Newesely, C., Tasser, E., Spadinger, P., and Cernusca, A.: Effects of land-use changes on snow gliding processes in alpine ecosystems, Basic Appl. Ecol., 1, 61–67, doi:10.1078/1439-1791-00009, 2000.

Panagos, P., Meusburger, K., Van Liedekerke, M., Alewell, C., Hiederer, R., and Montanarella, L.: Assessing soil erosion in Europe based on data collected through a European Network, Soil Sci. Plant Nutr., 1–15, doi:10.1080/00380768.2013.835701, 2014.

Parker, S. P.: McGraw-Hill Dictionary of Scientific and Technical Terms, published by The McGraw-Hill Companies, Inc., New York City, 2002.

Renard, K. G., Foster, G. R., Weesies, G. A., MCCool, D. K., and Yoder, D. C.: Predicting soil erosion by water; a guide to conservation planning with the revised universal soil loss equation (RUSLE), US Department of Agriculture, Agricultural Research Service, 404 pp., 1997.

Riesen, T., Zimmermann, S., and Blaser, P.: Spatial Distribution of 137CS in Forest SOils of Switzerland, Water Air Soil Poll., 114, 277–285, doi:10.1023/a:1005045905690, 1999.

Risse, L. M., Nearing, M. A., Nicks, A. D., and Laflen, J. M.: Error assessment in the Universal Soil Loss Equation, Soil Sci. Soc. Am. J., 57, 825–833, 1993.

Rogler, H. and Schwertmann, U.: Rainfall erosivity and isoerodent map of Bavaria, Z. Kulturtech. Flurber., 22, 99–112, 1981.

Schaub, M., Konz, N., Meusburger, K., and Alewell, C.: Application of in-situ measurement to determine 137Cs in the Swiss Alps, J. Environ. Radioact., 101, 369–376, 2010.

Schimmack, W. and Schultz, W.: Migration of fallout radiocaesium in a grassland soil from 1986 to 2001 – Part 1: Activity-depth profiles of ^{134}Cs and ^{137}Cs, Sci. Total Environ., 368, 853–862, 2006.

Schimmack, W., Bunzl, K., and Zelles, L.: Initial rates of migration of radionuclides from the Chernobyl fallout in undisturbed soils, Geoderma, 44, 211–218, 1989.

Schuller, P., Bunzl, K., Voigt, G., Ellies, A., and Castillo, A.: Global fallout ^{137}Cs accumulation and vertical migration in selected soils from South Patagonia, J. Environ. Radioact., 71, 43–60, doi:10.1016/s0265-931x(03)00140-1, 2004.

Schüpp, M.: Objective weather forecasts using statistical aids in Alps, Rivista Italiana Di Geofisica E Scienze Affini, 1, 32–36, 1975.

Shakhashiro, A. and Mabit, L.: Results of an IAEA intercomparison exercise to assess 137Cs and total 210Pb analytical performance in soil, Appl. Radiat. Isotopes, 67, 139–146, 2009.

Smith, S. J., Williams, J. R., Menzel, R. G., and Coleman, G. A.: Prediction of sediment yield from Southern Plains grasslands with the Modified Universal Soil Loss Equation, J. Range Manage., 37, 295–297, doi:10.2307/3898697, 1984.

Stanchi, S., Freppaz, M., Ceaglio, E., Maggioni, M., Meusburger, K., Alewell, C., and Zanini, E.: Soil erosion in an avalanche release site (Valle d'Aosta: Italy): towards a winter factor for RUSLE in the Alps, Nat. Hazards Earth Syst. Sci., 14, 1761–1771, doi:10.5194/nhess-14-1761-2014, 2014.

Sutherland, R. A.: Caesium-137 soil sampling and inventory variability in reference locations: A literature survey, Hydrol. Process., 10, 43–53, 1996.

US Department of Agriculture, S. C. S.: Procedure for computing sheet and rill erosion on project areas, Technical Release No. 51 (Rev. 2), Soil Conservation Service, Engineering Division, 1977.

Walling, D. E., Zhang, Y., and He, Q.: Models for deriving estimates of erosion and deposition rates from fallout radionuclide (caesium-137, excess lead-210, and beryllium-7) measurements and the development of user friendly software for model implementation, in: Impact of Soil Conservation Measures on Erosion Control and Soil Quality, IAEA-TECDOC-1665, Vienna, 11–33, 2011.

Wischmeier, W. H. and Smith, D. D.: Predicting rainfall-erosion losses from cropland east of the Rocky Mountains, Agriculture Handbook 282, US Department of Agriculture, Washington, D.C., 1965.

Wischmeier, W. H. and Smith, D. D.: Predicting Rainfall Erosion Losses – A Guide to Conservation Planning, USDA/Science and Education Administration, US. Govt. Printing Office, Washington, D.C., 58 pp., 1978.